Analysis of spontaneous bursting activity in random neural networks

Joël Tabak[CA] and Peter E. Latham[I]

Laboratory of Neural Control, Section on Developmental Neurobiology, Rm 3A50, Bldg 49, NIH Campus, NINDS, NIH, Bethesda, MD 20892; [I]Department of Neurobiology, University of California Los Angeles, Los Angeles, CA 90095-1763, USA

[CA]Corresponding Author: tabakszj@ninds.nih.gov

Received 19 April 2003; accepted 12 May 2003

DOI: 10.1097/01.wnr.0000082024.91120.20

Developing networks can generate bursting activity despite the absence of pacemaker cells and inhibitory synapses. Bursts are generated by positive feedback through excitatory connections and terminated by a slow depression of network excitability. Similar activity has been observed in cultures of spinal neurons containing inhibitory synapses. Is burst generation in these cultures operating according to the mechanism proposed for developing networks? To answer this question without perturbing the activity, we analyzed the burst pattern of individual neurons in active cultures. We observed a correlation between burst size and preceding interburst interval and a rapid rise and progressive decrease in firing rate during a burst. These findings are consistent with the mechanism of burst generation proposed for developing networks. *NeuroReport* 14:1445–1449 © 2003 Lippincott Williams & Wilkins.

Key words: Activity-dependent depression; Dissociated spinal culture; Positive feedback

INTRODUCTION

Rhythmic activity is widespread in the nervous system and is critical for functions such as respiration and locomotion. Rhythmogenesis often requires pacemaker cellular properties or depends on synaptic connectivity, particularly reciprocal inhibition of antagonist centers [1]. However, rhythmic, episodic activity has also been observed in disinhibited or developing networks in which $GABA_A$ and glycine receptors are either blocked or have excitatory effects [2]. Several modeling and experimental studies suggest that such rhythmic activity can be generated by hyper-excitable networks in the absence of pacemaker circuitry or cells. In these models, synchronized bursts of activity are generated through positive feedback within the network and terminated by a slow activity-dependent depression of network excitability [3–13]. It is not known whether such a mechanism participates in the operation of mature central pattern generators with functional inhibition.

The generality of this mechanism is exemplified by neuronal cultures in which the network connections are believed to be randomized [14]. Can this mechanism still apply in dissociated spinal cord cultures including both excitatory and inhibitory connectivity? Latham *et al.* [6] showed that network activity switched from steady firing at low rates to synchronized bursting when the number of endogenously active cells was decreased, without blocking inhibitory connections in the cultures. This behavior could be explained theoretically if neurons were subject to spike frequency adaptation, acting as a slow negative feedback process to terminate the bursts [5]. These results suggest that the same mechanism of burst generation implicated for excitatory networks could apply to a random network with functional inhibitory connections. However, although Latham *et al.* [5] showed how the number of intrinsically spiking cells affected network activity, they did not directly establish that the bursts observed in the dissociated cultures were terminated by a slow adaptation of network excitability, rather than another mechanism involving synaptic inhibition.

Therefore, the goal of the present work was to establish if bursting in these cultured networks exhibited properties characteristic of those observed in purely excitatory networks which would implicate a mechanism of rhythmogenesis based on recurrent excitation and slow activity-dependent network depression that recovers during the interburst interval. This scheme predicts that there is a statistical relationship between burst size and the length of the interburst interval [11,15] and that neuronal firing rate increases abruptly at the beginning of a burst, then decreases progressively. To verify these predictions, we analyzed the spike train patterns previously recorded [6] during bursting activity in these cultures. This method of analysis has the advantage of not perturbing network activity.

MATERIALS AND METHODS

We performed a new analysis of previously published data consisting of extracellular patch recordings performed on 27

cells in three cultures of dissociated spinal neurons, as described previously [6]. Although it was not possible to analyze more data, the results showed identical qualitative behavior in all three cultures. The recordings were made after the growth medium was replaced by a recording medium (saline solution), which decreased the number of endogeneously active cells, causing each culture to generate bursting activity [6]. It has been established previously that functional inhibitory synapses are present in this type of culture, both in growth and recording media [16,17], even though it is possible that inhibitory synapses were altered by the growth medium.

Data for each cell consisted of spike trains obtained from 5 min recordings (Fig. 1a). We first determined burst onset and termination. All the consecutive spikes separated by less than a minimum interburst interval (minIBI) were grouped in a burst. Because bursts are synchronized network events, the observed burst period does not vary much between cells [6]. Therefore, the minIBI should be common to all the cells from the same culture. To demonstrate that cells were bursting and determine their minIBI, we plotted their spike trains and return map as shown in Fig. 1. The return map is a plot of successive interspike intervals (ISI); that is, a plot of ISI_{n+1} *vs* ISI_n where ISI_n is the time interval between the nth and n + 1th spikes.

For a bursting cell, the histogram of ISIs is bimodal, which translates into a trimodal return map [18]. One mode is near the origin, corresponding to the short ISIs within a burst; a second is on the horizontal axis, corresponding to the intervals on each side of the first spike in a burst (large ISI_n and small ISI_{n+1}); and a third mode is on the vertical axis, corresponding to the intervals on each side of the last spike in a burst (small ISI_n and large ISI_{n+1}). We chose the value of the minIBI visually, so that it would separate the two modes near the horizontal axis for most cells. Small variations in the value of the minIBI did not affect the results.

We then computed the interburst intervals (IBI, difference between the onset time of the bursts and the termination time of the previous bursts) and the number of spikes of each burst. We discarded all bursts that comprised only one spike, because these spikes were likely to be just spontaneous cellular events. The IBIs were thus calculated as if these events did not occur. However, in 6/27 cells analyzed, most bursts comprised just a few spikes and the one-spike events were not a negligible part of the event distribution (not shown). These cells also exhibited the strongest spike frequency adaptation (median adaptation typically $> 25\%$, see below). For consistency, the single spike events were discarded and they were analyzed in the same way as the other cells (if the single-spike events were not discarded, a higher correlation between burst size and preceding IBI would have been found for these cells).

To measure the degree of association between burst size and interburst interval, we computed the Pearson correlation coefficient. We then constructed a *t*-statistic with $n-2$ degrees of freedom (n being the sample size) to assess the significance of the correlation. The null hypothesis (non-significant correlation) was rejected at the 5% level.

To quantify the degree of spike frequency adaptation for each cell, we first determined an adaptation coefficient for each burst containing ≥ 3 spikes. This coefficient was the median of the percentage change in instantaneous frequency (1/ISI), calculated for each pair of successive ISIs. The cellular adaptation coefficient was then defined as the median of all these coefficients. This coefficient represents the average decrease in frequency between two consecutives ISIs. Note the use of the median, rather than the mean, as the mean would have been more sensitive to outliers associated with very large or small ISIs. Also, statistics summarizing the results for all cells in a culture were expressed as the median and interquartile range (a distribution can be divided into four parts, each with equal probability, using

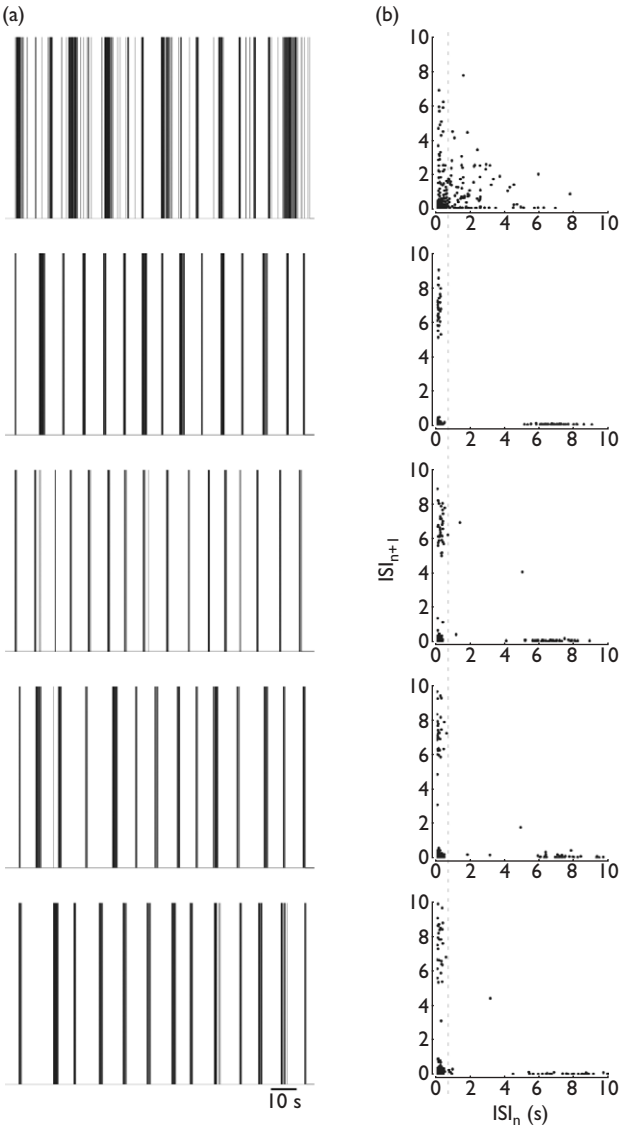

Fig. 1. Most cells of a given preparation are bursting regularly with similar bursting frequency. Spike train (**a**) and return map of ISIs (**b**) for five cells recorded consecutively. The plots in (b) were used to determine the minIBI value used for analysis (vertical dashed line, minIBI = 0.7 s for this preparation). The distribution of ISIs is similar in all the regularly bursting cells because bursts are population events. The horizontal clusters have smaller width than the vertical clusters, showing an increase between the first and last ISI in a burst, that is, a lower firing rate at the end of the bursts.

three points; if the three points are denoted Q_1, Q_2 and Q_3, then Q_2 is the median and Q_1–Q_3 is the interquartile range).

RESULTS

Bursting behavior and activity-dependent depression of excitability: As previously reported, most cells (20/27) burst regularly during the 5 min recording [6]. We plotted the spike trains and Return maps of ISIs to assess the regularity of bursting and measure the minIBI for each culture. This is shown in Fig. 1 for one culture. Of the five cells recorded from that culture, four were bursting regularly. The minIBI was < 1 s and clearly separated the two modes near the horizontal axis for all regularly bursting cells (Fig. 1b).

We then asked whether there was a relationship between IBI and burst size, with burst size measured as the number of spikes per burst. Figure 2a,b shows scatter plots of burst size versus preceding and following interval, respectively, for the same cell. This cell was typical in that it showed a positive correlation between burst size and preceding interval, but no correlation between burst size and following interval. Overall, 21/27 cells showed a significant correlation ($p < 0.05$) between burst size and preceding interval, although a minority 8/27 showed a significant correlation between burst size and following interval ($p < 0.05$), which was negative in two instances. These results are summarized in Fig. 2c for one culture and in Table 1 for all cultures. Similar results were obtained when burst duration (instead of number of spikes) was used as a measure of burst size, indicating that they are unlikely to be artifacts of anomalous spike trains.

Spike frequency adaptation: If bursts are controlled by a slow adaptation mechanism, the average spike frequency within the network should decrease during a burst until the burst stops. This is true whether the reduction of network excitability originates at the cellular level by decreasing impulse frequency (Fig. 6B of [5]) or at the synaptic level by a decrease in synaptic drive.

Examination of spike trains revealed a tendency to fire more slowly towards the end of a burst (Fig. 3a). This drop in frequency is further illustrated in Fig. 3b,c, where instantaneous frequency is plotted as a function of time during a burst. Typically, frequency rapidly reached a maximum at the beginning of a burst, and then continuously decreased, with the steepest decline at the beginning of the burst. For some cells, the initial steep phase was not apparent and the frequency drop was almost uniform during the whole burst, while some cells had a very sharp decrease initially and an almost flat plateau phase. This variability between cells could be due to differences of membrane properties and/or afferent connections. Despite this variability, all cells showed a decrease in spike frequency during the bursts; the frequency drop between first and last spikes in a burst was 60% on average (Table 1). The median adaptation coefficient (the median of the percentage drop between successive ISIs; see Materials and Methods), also shown in Table 1, confirms that the drop in frequency is not just occurring during the first spikes, otherwise this coefficient would be zero.

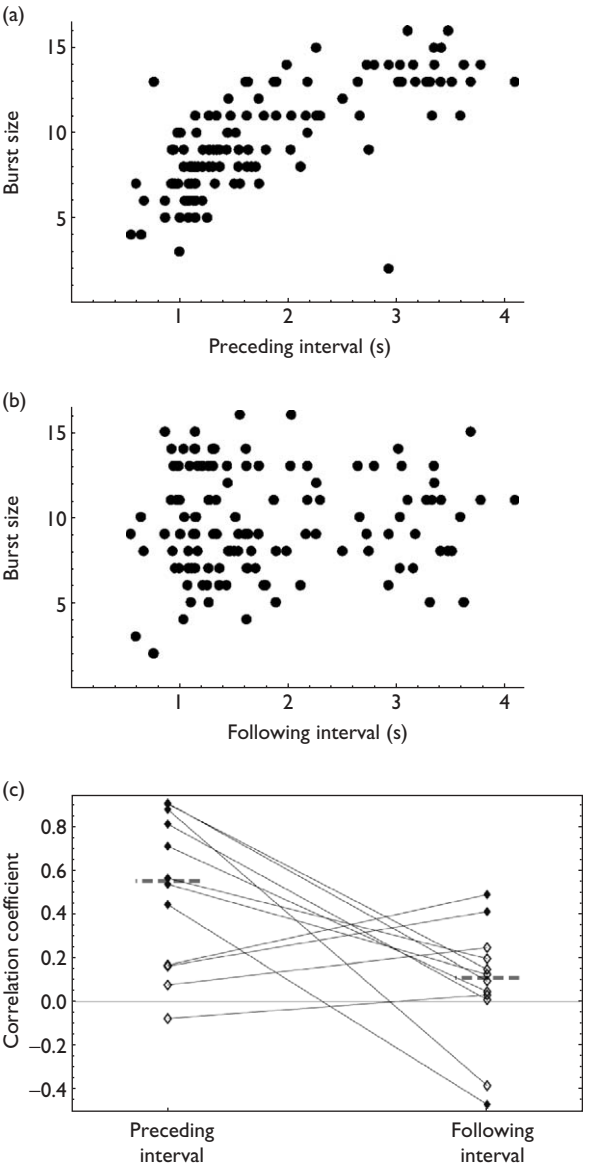

Fig. 2. Correlation patterns. (**a**) Scatter plot of burst size versus previous IBI for the bursting activity in one cell during a 5 min recording. There is a positive correlation between burst size and previous IBI ($r = 0.70$). (**b**) There is no correlation between burst size and following IBI ($r = 0.05$). (**c**) Values of the correlation coefficients between burst size and previous IBI (left) or following IBI (right) for the 12 cells recorded in one culture. Filled symbols: significant; open symbols: not significant; horizontal gray lines: median values of the correlation coefficients; pairs of values from the same cell are linked by dotted lines.

DISCUSSION

In the majority of cells we examined, burst size was positively correlated with the duration of the previous interburst interval. In addition, we found that the spike frequency began high at burst onset, and then decreased during the bursts. These findings are consistent with a mechanism of burst generation based on positive feedback recruitment and an activity-dependent depression of network excitability and recovery during the IBI.

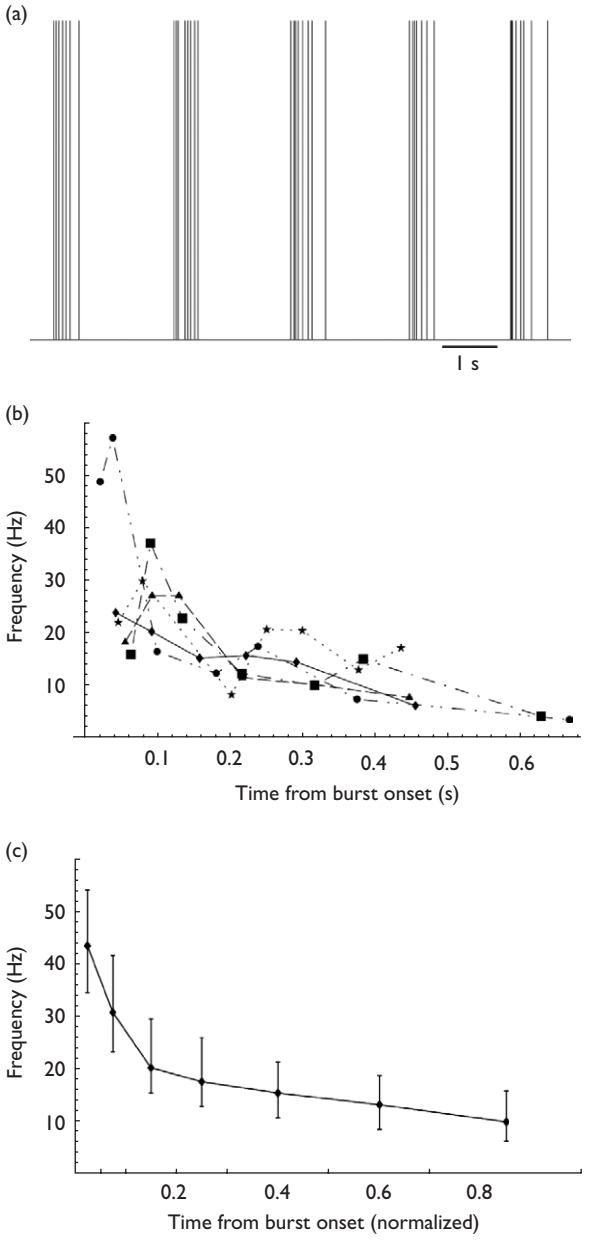

Fig. 3. Adaptation of spike frequency (same cell as Fig. 2). (**a**) Portion of spike train showing five bursts. (**b**) For each of these bursts, the instantaneous frequency (= 1/ISI) decreases with time measured from the first spike of the burst. (**c**) Time was normalized to average the instantaneous frequency over all bursts. For each time bin (delimited by two consecutive upward ticks on the horizontal axis), the median of all instantaneous frequencies occuring within the bin is represented. Error bars represent the interquartile range.

The positive correlation between burst size and the duration of the preceding IBI was significant for most cells (21/27) in all cultures. Four of the six cells that did not exhibit this correlation were bursting irregularly during their entire recording time. These cells might have been damaged or not well connected to the rest of the network. The majority of cells (19/27) showed no consistent correlation between burst size and following IBI. Of the eight cells that did, three were among the irregular bursters and in two the correlation was negative. Because bursts are synchronized network events, we conclude that the main pattern observed in these networks is a positive correlation between burst size and the length of the preceding, but not following, IBI.

This pattern of correlation suggests that bursts are terminated by an activity-dependent process which depresses network excitability until it is too low to sustain activity, the interburst interval being a period of recovery from this depression. Burst duration does not influence the length of the interval before the next burst, implying that network excitability is reset to the same value after each burst [11]. Therefore, the length of the silent phase determines the level of network excitability. All bursts do not start at the same level of excitability, because even though the network is capable of sustaining a burst after minimal recovery, a triggering event (for example, firing of a few cells due to spontaneous EPSPs [12]) is needed to start a burst.

If fast synaptic inhibition terminated the bursts before full depression, network excitability at the end of a burst would depend on the burst duration (a longer burst would depress network excitability more). In that case, a long burst would likely be followed by a long interval, so there would be a positive correlation between burst size and following interval. Such a correlation was indeed observed by Streit *et al.* [14] when inhibition was only partially blocked. Note that by synaptic inhibition we understand fast ionotropic transmission mediated by $GABA_A$ or glycine receptors, not the slow modulation of cellular excitability and synaptic transmission due to the activation of $GABA_B$ receptors, a possible mechanism of activity-dependent depression.

The immediate jump in firing frequency at the beginning of a burst, followed by a gradual decline in firing rate, suggest a bursting mechanism known as square-wave bursting [19]. According to this mechanism, a slow adaptation/depression process switches the network back and forth between silent and active states and is therefore responsible for the decrease in firing frequency during a burst. It is important to emphasize that fast synaptic inhibition may also limit firing rate during the bursts, and may be involved in burst termination. Nevertheless, it is unclear how synaptic inhibition alone would be able to allow for both a fast jump and a slow decrease in firing frequency during the bursts.

Collectively, our analysis of inter- and intra-burst timings suggests a slow activity-dependent depression of network excitability as the burst termination mechanism, although the data do not allow us to distinguish between a cellular or synaptic basis for the depression. Synaptic depression has been implicated in the activity of the developing chick spinal cord [10], hippocampal slices [9] and dissociated retinal networks [20]. Regulation of cellular excitability is thought to control bursts in neocortex [21], disinhibited rat spinal cultures [4] and possibly in the lamprey spinal cord [22].

Whole-cell recordings and pharmacology will be useful in order to eliminate the participation of inhibition in burst termination [9] and to determine the type of adaptation (synaptic or cellular) present in the network. For example, we could test for a cellular adaptation mechanism by

Table 1. Summary of the correlation and adaptation statistics obtained from each cultures.

	r (size *vs* preceding interval)	r (size *vs* next interval)	Total adaptation (%)[a]	Median adaptation (%)[b]
Experiment 1	0.40 [0.32–0.50] (4/5)	−0.15 [−0.23–0.0] (2/5)	59 [38–64]	5.9 [4.9–16]
Experiment 2	0.55 [0.16–0.84] (8/12)	0.11 [0.02–0.22] (3/12)	60 [58–71]	9.3 [5.8–17]
Experiment 3	0.42 [0.32–0.49] (9/10)	0.11 [−0.01–0.15] (3/10)	62 [57–69]	9.0 [6.8–18]

[a]Decrease in frequency between first and last ISI of a burst.
[b]Median decrease in frequency between successive ISIs in a burst.
Results are given as median over each cell of a culture, with the interquartile range indicated within square brackets.
The number of significant correlations over the number of cells analyzed is represented in parentheses.

blocking slow after-hyperpolarization currents. However, this may profoundly alter the network, as in disinhibited rat cord organotypic cultures [8] where blockade of cellular depression can unmask synaptic depression. It is therefore important to limit ourselves to manipulations that do not perturb the dynamical regime of the circuit. Our results show that a surprising amount can be learned about rhythm generation by simply analyzing the temporal structure of spike trains. This type of analysis might be usefully applied to *in vivo* recording where a more direct analysis of network mechanisms is impossible.

CONCLUSION

Together with the absence of pacemaker cells [6], our results suggest that the bursting activity observed in the mice spinal cord cultures is controlled by the interaction between recurrent excitation and activity-dependent decrease of excitability. They strengthen the hypothesis of a general mechanism of bursting activity in developing and hyper-excitable networks and indicate that this mechanism can operate in networks with inhibitory transmission [9,21,23]. This mechanism could therefore be a component of mature central pattern generators.

REFERENCES

1. Marder E and Calabrese RL. *Physiol Rev* **76**, 687–717 (1996).
2. O'Donovan MJ. *Curr Opin Neurobiol* **9**, 94–104 (1999).
3. Butts DA, Feller MB, Shatz CJ and Rokhsar DS. *J Neurosci* **19**, 3580–3593 (1999).
4. Darbon P, Scicluna L, Tscherter A and Streit J. *Eur J Neurosci* **15**, 671–683 (2002).
5. Latham PE, Richmond BJ, Nelson PG and Nirenberg S. *J Neurophysiol* **83**, 808–827 (2000).
6. Latham PE, Richmond BJ, Nirenberg S and Nelson PG. *J Neurophysiol* **83**, 828–835 (2000).
7. Maeda E, Robinson HPC and Kawana A. *J Neurosci* **15**, 6834–6845 (1995).
8. Rozzo A, Ballerini L, Abbate G and Nistri A. *J Neurophysiol* **88**, 676–691 (2002).
9. Staley KJ, Longacher M, Bains JS and Yee A. *Nature Neurosci* **1**, 201–209 (1998).
10. Tabak J, Senn W, O'Donovan MJ and Rinzel J. *J Neurosci* **20**, 3041–3056 (2000).
11. Tabak J, Rinzel J and O'Donovan MJ. *J Neurosci* **21**, 8966–8978 (2001).
12. Traub RD and Dingledine R. *J Neurophysiol* **64**, 1009–1018 (1990).
13. van Vreeswijk C and Hansel D. *Neural Comput* **13**, 959–992 (2001).
14. Streit J, Tscherter A, Heuschkel MO and Renaud P. *Eur J Neurosci* **14**, 191–202 (2001).
15. Grzywacz N and Sernagor E. *Vis Neurosci* **7**, 229–241 (2000).
16. Ransom BR, Christian CN, Bullock PN and Nelson PG. *J Neurophysiol* **40**, 1151–1162 (1977).
17. Ransom BR, Bullock PN and Nelson PG. *J Neurophysiol* **40**, 1163–1177 (1977).
18. Dekhuijzen AJ and Bagust J. *J Neurosci Methods* **67**, 141–147 (1996).
19. Rinzel J and Ermentrout GB. Analysis of neural excitability and oscillations. In: Koch C and Segev I (eds). *Methods in Neuronal Modeling*. Cambridge: MIT Press; 1998.
20. Harris RE, Coulombe MG and Feller MB. *J Neurophysiol* **88**, 188–195 (2002).
21. Sanchez-Vives MV and McCormick DA. *Nature Neurosci* **3**, 1027–1034 (2000).
22. Hellgren Kotaleski J, Lansner A and Grillner S. *Biol Cybern 81*, 299–315 (1999).
23. Tscherter A, Heuschkel MO, Renaud P and Streit J. *Eur J Neurosci* **14**, 179–190 (2001).

Acknowledgements: We thank Dr Michael O'Donovan for his extensive review of the manuscript. We also thank Dr Phillip Nelson for discussing important aspects of the cell cultures.